

## Supplementary Information

### [Mutational cooperativity of TET2 and RHOA disrupts peripheral T-cell homeostasis](#)

Shengbing Zang<sup>1,2\*</sup>, Jia Li<sup>1,2\*</sup>, Haiyan Yang<sup>3\*</sup>, Hongxiang Zeng<sup>1,2</sup>, Wei Han<sup>1,2</sup>, Jixiang Zhang<sup>1,2,4</sup>, Minjung Lee<sup>1,2</sup>, Margie Moczygemba<sup>5</sup>, Sevinj Isgandarova<sup>5</sup>, Yaling Yang<sup>6</sup>, Yubin Zhou<sup>7,8</sup>, Anjana Rao<sup>9,10,11</sup>, M. James You<sup>6,12#</sup>, Deqiang Sun<sup>1,2,#</sup>, Yun Huang<sup>1,2,#</sup>

1. Center for Epigenetics & Disease Prevention, Institute of Biosciences and Technology, Texas A&M University, Houston, TX 77030
2. Department of Molecular & Cellular Medicine, College of Medicine, Texas A&M University, College Station, TX 77843
3. Department of Lymphoma, Zhejiang Cancer Hospital, Hangzhou, China
4. Department of Gastroenterology, Renmin Hospital of Wuhan University, Wuhan, Hubei, China
5. Center for Infectious and Inflammatory Diseases, Institute of Biosciences and Technology, Texas A&M University, Houston, TX 77030
6. Department of Hematopathology, The University of Texas MD Anderson Cancer Center, Houston, TX 77030
7. Center for Translational Cancer Research, Institute of Biosciences and Technology, Texas A&M University, Houston, TX 77030
8. Department of Medical Physiology, College of Medicine, Texas A&M University, College Station, TX 77843
9. Division of Signaling and Gene Expression, La Jolla Institute for Allergy and Immunology, La Jolla, CA 92037
10. Sanford Consortium for Regenerative Medicine, La Jolla, CA 92037 Department of Pharmacology, University of California, San Diego, La Jolla, CA 92093
11. Moores Cancer Center, University of California, San Diego, La Jolla, CA 92093
12. The University of Texas MD Anderson Cancer Center UT Health Graduate School of Biomedical Sciences, Houston, TX 77030

\* These authors contributed equally to the work

# Correspondence: # Correspondence: [mjamesyou@mdanderson.org](mailto:mjamesyou@mdanderson.org), [dsun@ibt.tamhsc.edu](mailto:dsun@ibt.tamhsc.edu); [yun.huang@ibt.tamhsc.edu](mailto:yun.huang@ibt.tamhsc.edu) (lead contact)

### [Correspondence information:](#)

#### [Yun Huang](#)

[Mailing address: Room 404, 2121 W. Holcombe Blvd, Houston, TX 77030](#)

[Email: yun.huang@ibt.tamhsc.edu](mailto:yun.huang@ibt.tamhsc.edu)

[Phone: 713-677-7484](tel:713-677-7484)

[The authors have declared that no conflict of interest exists](#)

## SUPPLEMENTARY EXPERIMENTAL PROCEDURES

### Animals

All animals were housed at the Institute of Biosciences and Technology, Texas A&M University. All animal procedures were conducted in accordance with the Guidelines for the Care and Use of Laboratory Animals and were approved by the Institutional Animal Care and Use Committees at Texas A&M Institute of Biosciences and Technology. Tet2<sup>-/-</sup> mice have been described previously (Ko et al., 2011). C57BL/6 and TCR $\alpha$ <sup>-/-</sup> mice were purchased from the Jackson Laboratory.

### Plasmid construction and retrovirus transduction

A cDNA fragment encoding FLAG-tagged murine *RhoA* was synthesized (Integrated DNA Technologies) and cloned into the MSCV-IRES-GFP vector between the restriction sites of XhoI and EcoRI. The RhoA G17V mutation was introduced by PrimeStar Mutagenesis Basal kit (Takara). HA-tagged FoxO1 gene was subcloned from pGFP-N1 FoxO1 (Addgene 17551) into the MSCV-IRES-mCherry vector between the restriction sites of BamHI and XhoI. All the plasmids were verified by Sanger sequencing (Eurofins MWG Operon LLC). The correct plasmids were prepared using PureLink HiPure Plasmid Maxiprep kit (Thermo Fischer Scientific).

Retroviruses encoding murine RhoA (WT or G17V mutant) or FoxO1 were generated using MSCV and EcoPack plasmids transfected into the potent retrovirus packaging cell line, Plat-E (Cell Biolabs). Retrovirus-containing supernatants were collected from transfected Plat-E cells and then concentrated using ultracentrifugation (Beckman SW28 rotor, 20,000 rpm for 2 hr at 4°C). Concentrated retroviruses were re-suspended, aliquoted and stored in -80°C up to 2 months.

After 12-24 hr stimulation of T cells (CD4<sup>+</sup> or CD8<sup>+</sup>), concentrated retroviruses at optimized titers, along with polybrene (6  $\mu$ g/ml, EMD Millipore), were added to cultured T cells, followed by centrifugation (2000 rpm at 37°C for 90 min). The transduction efficiency of retrovirus was examined by flow cytometry 24-48 hrs after transduction.

### Histological and Immunohistochemical (IHC) staining of mouse tissues

All tissues or organs from mice were harvested and fixed in 4% formaldehyde for 24 hrs. The specimens were then treated with gradient alcohol dehydration, and tissue blocks were embedded in paraffin. 4  $\mu$ m-thick slices were cut for Hematoxylin and Eosin (H&E) staining. IHC staining were performed using the ImmPRESSTM Polymer Detection Systems (Vector Laboratories) according to the manufacturer's instructions. Sections were deparaffinized and rehydrated in xylene and ethanol grades. To block endogenous peroxidase activity, sections were incubated in 3% H<sub>2</sub>O<sub>2</sub> for 15 min. Heat-induced

epitope retrieval was achieved by incubating slides in 10 mM sodium citrate, pH 6.0 (Vector Laboratories) in a pressure cooker for 4 min with full pressure. Sections were blocked with 2.5% normal goat or horse serum (Vector Laboratories) for 30 min and incubated with primary antibodies with optimized concentration (anti-CD3 (Abcam ab16669): 1:200; anti-B220 (Abcam ab10558): 1:400; anti-CD35 (Biorbyt orb308735): 1:400; anti-FoxO1 (Cell Signaling Technology 2880P): 1:100) for 1 h followed by three washes with phosphate buffer saline (PBS, 0.5% Tween 20). The slides were incubated with ImmPRESSTM HRP Anti-Rabbit/rat IgG (Vector Laboratories) for 1 h, followed by 3-3' diaminobenzidine (DAB), and counterstained with hematoxylin. Negative control sections were incubated with preimmune serum (Vector Laboratories). All the prepared slides were analyzed under a Nikon upright microscope.

### **Isolation and differentiation of naïve CD4<sup>+</sup> T cell**

Naïve CD4<sup>+</sup> T cells were isolated using a naïve CD4<sup>+</sup> T cell isolation kit (Miltenyi Biotec). These cells were cultured on goat-anti-hamster IgG coated plate for 12-24 hrs in standard T cell culture medium with anti-CD3 (200 ng/ml) and anti-CD28 (200 ng/ml) followed by retroviral transduction. T cells were differentiated toward Th17 in the presence of TGF- $\beta$  (3 ng/ml), IL-6 (30 ng/ml), IL-23 (20 ng/ml), anti-IFN $\gamma$  (33 ng/ml), anti-IL-4 (10 ng/ml) for 2-3 days. Tregs were differentiated in the presence of anti-IL-4 (10 ng/ml), anti-IFN $\gamma$  (33 ng/ml), anti-IL-12 (10 ng/ml), IL-2 (100 U/ml), TGF- $\beta$  (3 ng/ml) for 3-5 days. The differentiation efficiency was examined by flow cytometry analysis of immunostaining for IL-17a (Th17) and Foxp3 (Treg).

### **Flow cytometry and cell sorting**

Cells were re-suspended in FACS buffer (PBS with 1% BSA, 2 mM EDTA) and incubated with Fc blocker for 10 min on ice. After wash with FACS buffer, cells were incubated with desired antibodies at optimal concentrations for 20 min on ice in the dark. Cells were then washed with FACS buffer twice and re-suspended in 200  $\mu$ l FACS buffer for flow cytometry analysis (LSRII, BD biosciences). For intracellular staining, GFP<sup>+</sup> cells were first sorted using a BD FACSAria Fusion instrument and stained with surface marker as described above, treated with cell fixation/ permeabilization kit (BD Biosciences) and then incubated with antibodies for desired intracellular markers. For Foxp3 staining, cells were treated with fixation/ permeabilization reagents from eBioscience followed incubation with an anti-Foxp3 antibody (eBioscience 12-5773-80). All antibodies were purchased from BioLegend, eBioscience or BD Biosciences. The following monoclonal antibodies conjugated with phycoerythrin (PE), PerCP-Cy5.5, PE-Cy7, allophycocyanin (APC), eFluor 450, APC-Cy7, Alexa Fluor 700, or Pacific Blue were used: CD4 (clone GK1.5, Biolegend 100438), CD8a (clone 53-6.7, Biolegend 100734), Ki-67 (clone SolA15, eBioscience 48-5698-82), Thy1.1 (clone HIS51, eBioscience 17-0900-82), Thy1.2 (clone 53-2.1, eBioscience 48-0902-82), Fas (clone 15A7, eBioscience 12-0951-83), GL-7 (clone GL7, Biolegend

144614), CD44 (clone IM7, Biolegend 103020), IL-17a (clone TC11-18H10.1, Biolegend 506919), Foxp3 (clone FJK-16S, eBioscience 12-5773-80), Bcl-6 (clone BCL-DWN, eBioscience 17-5453-80), INF- $\gamma$  (clone XMG1.2, eBioscience 12-7311-81). CXCR-5 staining was performed using three step staining protocol (Chen et al., 2014). NucRed Live 674 (Thermo Fisher Scientific) was used to examine cell death. Annexin V-pacific Blue (Biolegend) was used to assess the apoptotic status of cells. CellTrace Far Red (Thermo Fisher Scientific) was applied to probe the cell proliferation and proliferation index was calculated following the manufacturer's instructions. Cell cycle was assessed by 7-AAD (Tonbo Biosciences) and BrdU (Biolegend) staining. Flow cytometry analysis was performed using LSRII (BD Biosciences) and data were analyzed using the FlowJo software. Cell sorting were performed using a BD FACSAria Fusion instrument.

### **ELISA for serum IFN- $\gamma$ measurement**

The serum IFN-  $\gamma$  was measured by Mouse IFN gamma ELISA Ready-set-go kit from eBioscience (88-7314-22) following the manufacturer's instructions.

### **Cytospin and confocal imaging**

*In vitro* cultured CD4<sup>+</sup> T cells were deposited using Cytospin cytocentrifuge followed by fixation with 4% paraformaldehyde/ PBS for 15 mins. Cells were permeabilized in 0.2% Triton X-100/ PBS for 15 min and blocked with 1% BSA and 0.05% Tween in PBS for 1 hr at room temperature (RT). Primary antibodies were diluted in the blocking solution and incubated with cells for 1 hr at RT followed by 3 times wash with PBS. The secondary antibody was diluted in the blocking solution and incubated with cells at RT for 1 hr. Cells were further washed with PBS for 3 times and incubated with ProLong Gold Antifade Mountant with DAPI (ThermoFisher Scientific) for further imaging analysis. Confocal images were acquired using a Nikon A1+ confocal imaging system.

### **Real-time RT-PCR**

RNA was isolated from cell lysates using RNeasy mini kit (Qiagen) per manufacturer's instructions, followed by reverse transcription using an AmfiRivert Platinum One cDNA Synthesis Master Mix (GenDEPOT). Diluted cDNA was analyzed by real-time PCR using Roche LightCycler 96 real-time PCR system (Roche) and amfiSure qGreen Q-PCR Master Mix reagents (GenDEPOT). Data were analyzed using the LightCycler software. The gene expression level was normalized to Gapdh. Primer sequences used for real-time RT-PCR were listed below:

*Ii-6* forward: ATTTGTGTGCTGAAGGAGGC

*Ii-6* reverse: AAAGGACAGGATGTTGCAGG

*Rorc* forward: CCGCTGAGAGGGCTTCAC

*Rorc* reverse: TGCAGGAGTAGGCCACATTACA

*TGFβ* forward: ACCATGCCAACTTCTGTCTG

*TGFβ* reverse: CGGGTTGTGTTGGTTGTAGA

### **A dot-blot assay to quantify genomic 5hmC and 5mC**

Dot blot assays were performed as described previously (Ko et al., 2010). Briefly, purified genomic DNA was denatured in 0.4 M NaOH, 10 mM EDTA at 95 °C for 10 min, followed by neutralization with ice-cold 2 M ammonium acetate (pH 7.0). Two-fold serial dilutions of the denatured DNA samples were spotted on a nitrocellulose membrane in an assembled Bio-Dot apparatus (Bio-Rad) according to the manufacturer's instructions. A synthetic oligonucleotide with a known amount of 5hmC was used as standard (Huang et al., 2010; Ko et al., 2010). The membrane was washed with 2x SSC buffer, air-dried and vacuum-baked at 80°C for 2 hr. The dried membrane was blocked with 5% non-fat milk for 1 hr and incubated with an anti-5hmC antibody (1:5000, Active Motif 39769) for 1 hr at 4°C, followed by incubation with horseradish peroxidase-conjugated anti-rabbit IgG secondary antibody (1:10,000; Sigma). The membrane was visualized by West-Q Pico Dura ECL Solution (GenDEPOT). To ensure equal loading of total DNA on the membrane, the same blot was stained with 0.02% methylene blue in 0.3 M sodium acetate (pH 5.2).

### **Western blotting**

Cells were lysed with RIPA buffer (150 mM NaCl, 50 mM Tris-HCl, pH 8.0, 1% Triton X-100, 0.5% sodium deoxycholate and 0.1% SDS) supplemented with protease inhibitor cocktail (GenDEPOT) and incubated on ice for 20 min. Cell debris was removed by centrifuging at 12,000 rpm for 10 min at 4°C. The protein concentration was measured by a Pierce BCA protein assay kit (Thermo Fisher Scientific). Samples were mixed with SDS sample buffer at 95°C for 10 min. Whole cell lysates were resolved on 10% or 15% SDS-PAGE and transferred onto nitrocellulose membranes. Proteins were detected by immunoblotting in TBST (150 mM NaCl, 10 mM Tris-Cl, pH 8.0, 0.5% Tween-20) containing 5% low-fat milk followed by incubation with primary antibodies listed below at RT for 1 hr. Then the membrane was incubated with HRP-conjugated secondary antibodies (goat anti-mouse IgG HRP, Sigma) and proteins were detected by using the West-Q Pico Dura ECL kit (GenDEPOT).

#### *Primary antibodies used for immunoblotting experiments:*

Abcam: Anti-Tet2 (ab124297): 1:500;

Sigma: Anti-Flag (F1804): 1:1000; Anti-Gapdh (G9545): 1:10,000;

Santa Cruz Biotechnology: Anti-Cleaved Caspase 3 (sc-373730): 1:500; Anti-p21 (sc-6246): 1:500;

Anti-Cyclin D1 (sc-8396): 1:500; Anti-HA (sc-7392): 1:1000

Cell Signaling Technology: Anti-FoxO1 (2880): 1:1000; Anti-phosphorylated FoxO1 (9464): 1:500; Anti-Akt (4691): 1:1000; Anti-phosphorylated Akt (4058): 1:500; Anti-Mst1 (3682): 1:1000; Anti-phosphorylated Mst1 (3681): 1:500

## SUPPLEMENTARY TABLES

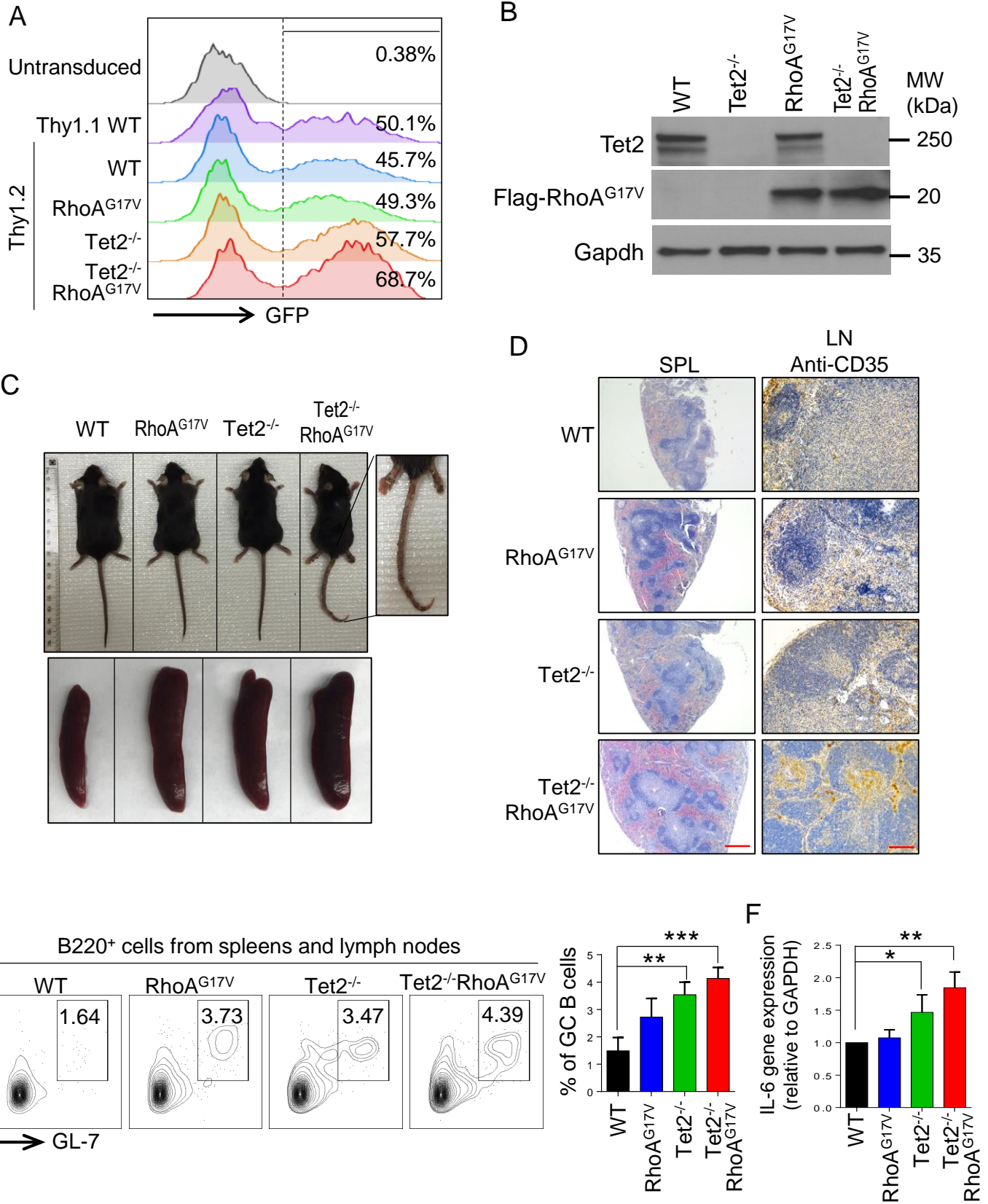
**Table S1:** List of differentially expressed genes (DEGs) (8 sheets)

**Table S2:** Summary of mutation status (TET2/RHOA) and FOXO1 IHC staining results in AITL patients (2 sheets)

## References

- Chen, R., Belanger, S., Frederick, M.A., Li, B., Johnston, R.J., Xiao, N., Liu, Y.C., Sharma, S., Peters, B., Rao, A., *et al.* (2014). In vivo RNA interference screens identify regulators of antiviral CD4(+) and CD8(+) T cell differentiation. *Immunity* *41*, 325-338.
- Huang, Y., Pastor, W.A., Shen, Y., Tahiliani, M., Liu, D.R., and Rao, A. (2010). The behaviour of 5-hydroxymethylcytosine in bisulfite sequencing. *PLoS One* *5*, e8888.
- Ko, M., Bandukwala, H.S., An, J., Lamperti, E.D., Thompson, E.C., Hastie, R., Tsangaratou, A., Rajewsky, K., Koralov, S.B., and Rao, A. (2011). Ten-Eleven-Translocation 2 (TET2) negatively regulates homeostasis and differentiation of hematopoietic stem cells in mice. *Proc Natl Acad Sci U S A* *108*, 14566-14571.
- Ko, M., Huang, Y., Jankowska, A.M., Pape, U.J., Tahiliani, M., Bandukwala, H.S., An, J., Lamperti, E.D., Koh, K.P., Ganetzky, R., *et al.* (2010). Impaired hydroxylation of 5-methylcytosine in myeloid cancers with mutant TET2. *Nature* *468*, 839-843.

Figure S1



**Supplementary Figure 1, related to Figure 1. Recipient mice transferred with Tet2<sup>-/-</sup>RhoA<sup>G17V</sup> T cells displayed inflammatory-like phenotype. [Data were shown as mean ± S.D.; \\* p < 0.05, \\*\\* p < 0.01, \\*\\*\\* p < 0.001.](#)**

**(A)** Quantification of retroviral transduction efficiency. Thy1.1 and WT or Tet2<sup>-/-</sup> Thy1.2 T cells were transduced with retroviruses encoding pMSCV-IRES-GFP or pMSCV-Flag-RhoA<sup>G17V</sup>-IRES-GFP.

**(B)** Immunoblot analysis confirming the deletion of Tet2 and successful transduction of MSCV-Flag-RhoA<sup>G17V</sup>-IRES-GFP in transduced T cells. Gapdh was as loading control amount the four indicated groups (WT, RhoA<sup>G17V</sup>, Tet2<sup>-/-</sup>, or Tet2<sup>-/-</sup>RhoA<sup>G17V</sup>).

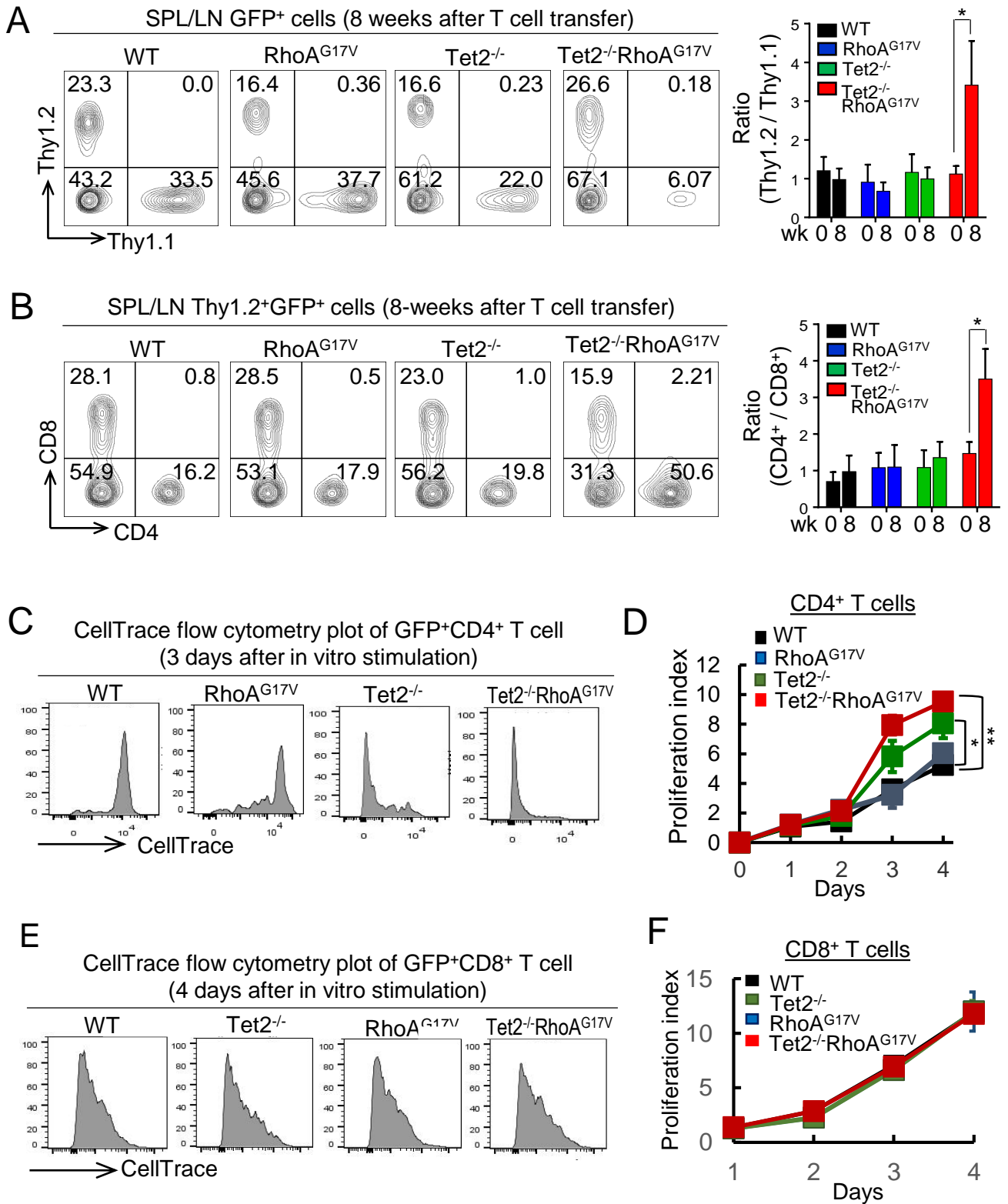
**(C)** Representative graphs of recipient mice transduced with indicated T cells at 20 weeks after adoptive transfer. *Top*, Recipient mice transferred with Tet2<sup>-/-</sup>RhoA<sup>G17V</sup> T cells showed a smaller size and skin ulcers on ear/paw/tail (enlarged panel on the right). Live mice also showed frequent self-grooming behavior, indicating itching and uncomfortable symptoms in mice. *Bottom*, spleens isolated from recipient mice showed no obvious difference in size.

**(D)** H&E staining of spleens (SPL, *left*, scale bar: 500 μm) and IHC staining of anti-CD35 in typical lymph nodes (LN, *right*, scale bar: 100 μm) isolated from recipient mice transferred WT, RhoA<sup>G17V</sup>, Tet2<sup>-/-</sup>, and Tet2<sup>-/-</sup>RhoA<sup>G17V</sup> T cells (20 weeks after adoptive transfer).

**(E)** Flow cytometry analysis on germinal center B cells in the indicated groups of recipient mice. *Left*, representative flow cytometry plots of B220<sup>+</sup>Fas<sup>+</sup>GL-7<sup>+</sup> cells in spleens and lymph nodes isolated from recipient mice. *Right*, quantification of the percentages of germinal center B (GCB) cells (n = 3 mice, [one experiment](#)). Statistical analysis was performed using the [ANOVA with Dunnett's post hoc correction](#).

**(F)** Quantitative analysis of *IL-6* expression by RT-PCR in T cells isolated from recipient mice at 20 weeks after transfer. The expression level of *IL-6* was normalized to that of *Gapdh* (n = 3 mice, [one experiment](#)). Statistical analysis was performed using the [ANOVA with Dunnett's post hoc correction](#).

# Figure S2



**Supplementary Figure 2, related to Figure 2. Tet2 loss and RhoA<sup>G17V</sup> expression mostly affect the proliferation of CD4<sup>+</sup> T cells, but not CD8<sup>+</sup> T cells. [Data were shown as mean ± S.D.; \\* p < 0.05, \\*\\* p < 0.01, \\*\\*\\* p < 0.001.](#)**

**(A)** *Left*, analysis of GFP-positive Thy1.1<sup>+</sup> and Thy1.2<sup>+</sup> T cell populations from the spleens and lymph nodes in recipient mice 8 weeks after adoptive transfer. Tet2<sup>-/-</sup> RhoA<sup>G17V</sup> Thy1.2<sup>+</sup> T cells displayed the strongest growth advantage over Thy1.1<sup>+</sup> T cells. *Right*, the statistical analysis of the ratio of GFP gated Thy1.2<sup>+</sup> and Thy1.1<sup>+</sup> T cells before (week 0) and 8 weeks after adoptive T cell transfer into the recipient mice (n = 3 mice, [three independent experiments](#); two-tailed Student's *t*-test).

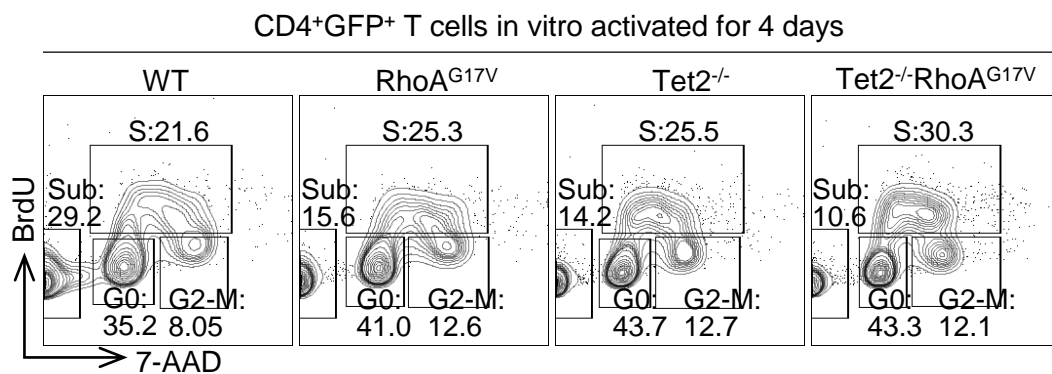
**(B)** *Left*, analysis of Thy1.2 and GFP double positive CD4<sup>+</sup> and CD8<sup>+</sup> T cells from the spleens and lymph nodes of recipient mice 8 weeks after adoptive transfer. *Right*, the statistical analysis of spleen and lymph node Thy1.2 and GFP double positive CD4<sup>+</sup> to CD8<sup>+</sup> T cell ratio at indicated time points after T cell transfer (n = 3 mice, [three independent experiments](#); two-tailed Student's *t*-test).

**(C and E)** CellTrace proliferation assay to quantify the proliferation of *in vitro* activated GFP<sup>+</sup> CD4<sup>+</sup> **(C)** and GFP<sup>+</sup> CD8<sup>+</sup> **(E)** T cells among four experimental groups (WT, RhoA<sup>G17V</sup>, Tet2<sup>-/-</sup>, or Tet2<sup>-/-</sup>RhoA<sup>G17V</sup>).

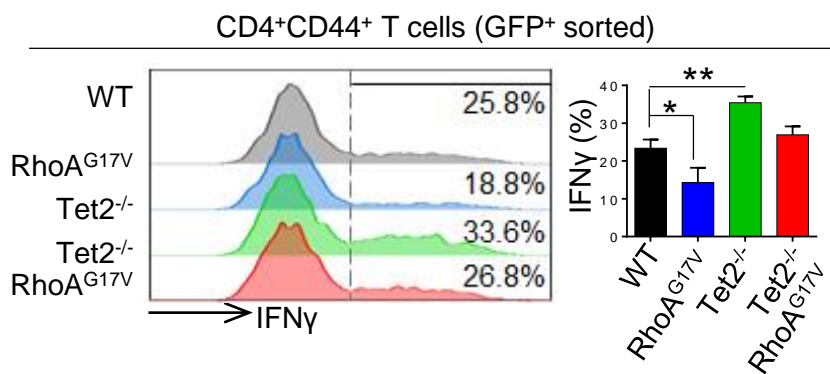
**(D, F)** Statistical analysis of proliferation index calculated from CellTrace proliferation assay over the time of stimulation of GFP<sup>+</sup>CD4<sup>+</sup> **(D)** and GFP<sup>+</sup>CD8<sup>+</sup> T **(F)** cells (WT, RhoA<sup>G17V</sup>, Tet2<sup>-/-</sup>, and Tet2<sup>-/-</sup>RhoA<sup>G17V</sup>; n = 3 independent experiments). Data were shown as mean ± S.D.; \* p < 0.1, \*\* p < 0.05 (two-tailed Student's *t*-test).

Figure S3

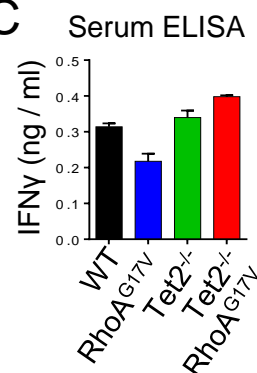
A



B

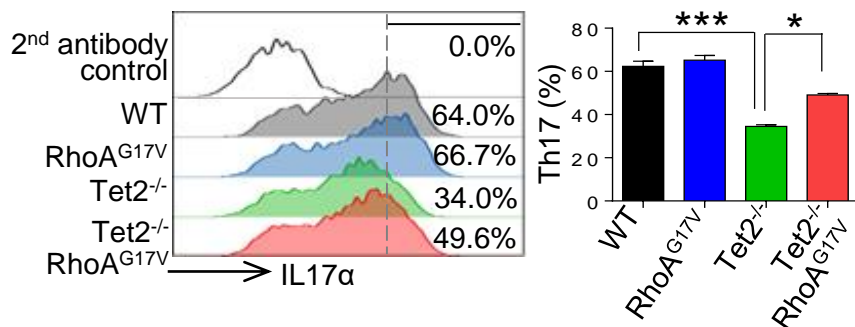


C

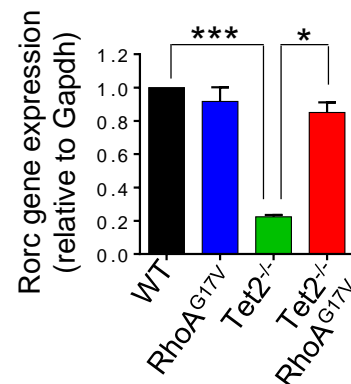


D

Naïve CD4<sup>+</sup> T cells in vitro differentiated to Th17 for 2 days (GFP<sup>+</sup> sorted)

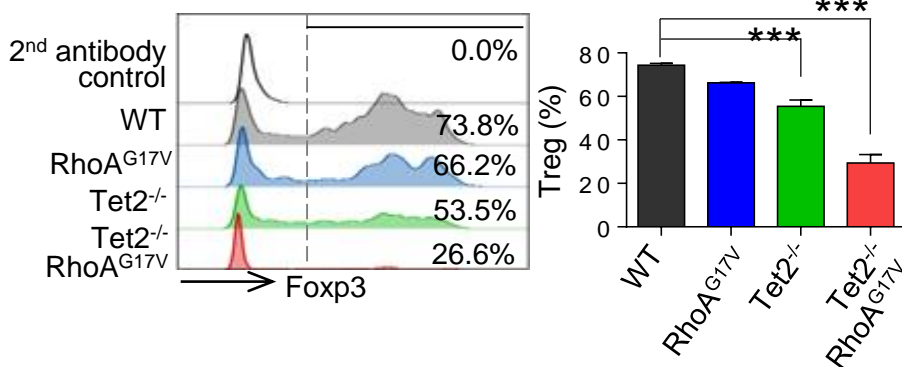


E

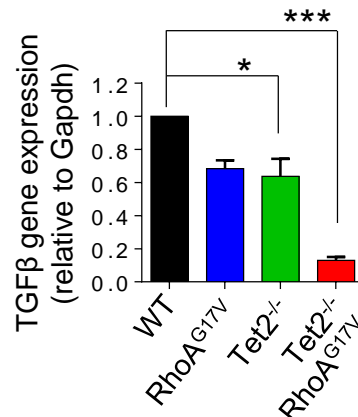


F

Naïve CD4<sup>+</sup> T cells in vitro differentiated to Treg for 3 days (GFP<sup>+</sup> sorted)



G



**Supplementary Figure 3, related to Figure 3. Tet2<sup>-/-</sup>RhoA<sup>G17V</sup> CD4<sup>+</sup> T cells exhibit alterations in cell cycle and biased polarization during *in vitro* differentiation.**

**Data were shown as mean ± S.D.; \* p < 0.05, \*\* p < 0.01, \*\*\* p < 0.001.** Statistical analysis was performed using the [ANOVA with Dunnett's post hoc correction](#).

**(A)** Cell cycle analysis with immunostaining for 7-AAD and BrdU in *in vitro* activated, GFP gated CD4<sup>+</sup> T cells at day 4 in the four indicated experimental groups (WT, RhoA<sup>G17V</sup>, Tet2<sup>-/-</sup>, or Tet2<sup>-/-</sup>RhoA<sup>G17V</sup>).

**(B)** Flow cytometry analysis of INF-γ in GFP<sup>+</sup> sorted CD4<sup>+</sup>CD44<sup>+</sup> T cells isolated from recipient mice 8 weeks after adoptive T cell transfer (WT, RhoA<sup>G17V</sup>, Tet2<sup>-/-</sup>, or Tet2<sup>-/-</sup>RhoA<sup>G17V</sup>). *Left*, representative flow cytometry plots; *Right*, Quantification of flow cytometry analysis results (n = 3 mice, [one experiment](#)).

**(C)** Measurement of serum INF-γ levels by ELISA in recipient mice 8 weeks after adoptive T cell transfer (WT, RhoA<sup>G17V</sup>, Tet2<sup>-/-</sup>, or Tet2<sup>-/-</sup>RhoA<sup>G17V</sup>; n = 3 mice, [one experiment](#)).

**(D, F)** Flow cytometry analysis on the efficiency of naïve CD4<sup>+</sup> T cells differentiated toward Th17 cells **(D)** or Tregs **(F)** *in vitro*. Naïve CD4<sup>+</sup> T cells were isolated from WT and Tet2<sup>-/-</sup> mice followed by transduction with a retrovirus encoding GFP or RhoA<sup>G17V</sup>-IRES-GFP; and then differentiated into Th17 and Treg cells with the corresponding polarizing cytokines as described in the methods. GFP<sup>+</sup> cells from each group were sorted prior to the analysis. *Left*, representative flow cytometry plots for each group of *in vitro* differentiated T cells; *Right*, Quantification of flow cytometry analysis results (n = 3 independent experiments).

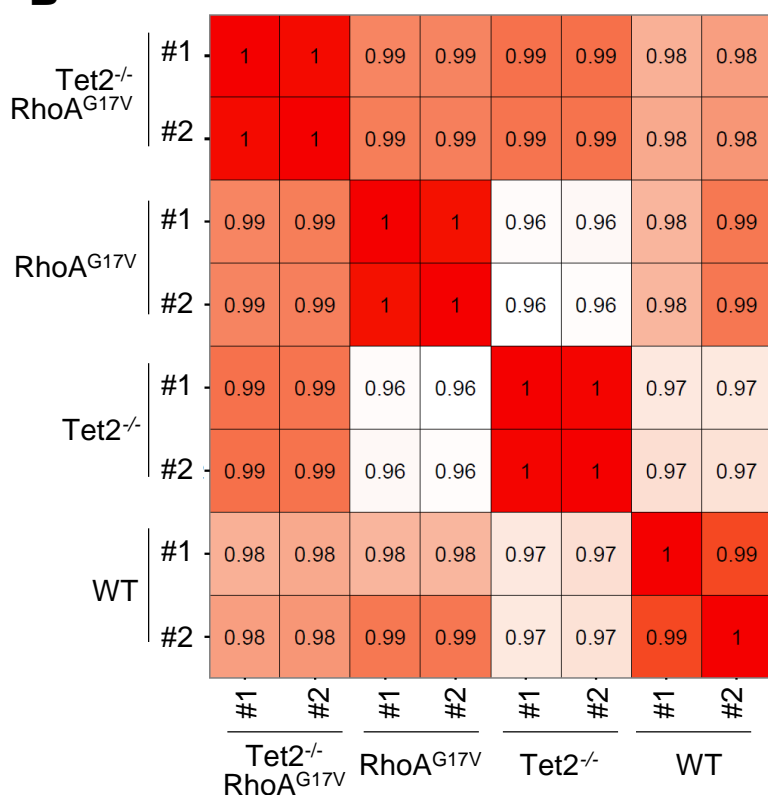
**(E, G)** Quantification of gene expression by real-time RT-PCR. The analyzed genes encode Rorγt (Rocr) **(E)** or TGFβ **(G)** during *in vitro* differentiation of naïve CD4<sup>+</sup> T cells (GFP<sup>+</sup> cells from each group were sorted prior to the analysis; WT, RhoA<sup>G17V</sup>, Tet2<sup>-/-</sup>, and Tet2<sup>-/-</sup>RhoA<sup>G17V</sup>; n = 3 independent experiments) toward the Th17 **(E)** or Treg lineage **(G)**, respectively.

Figure S4

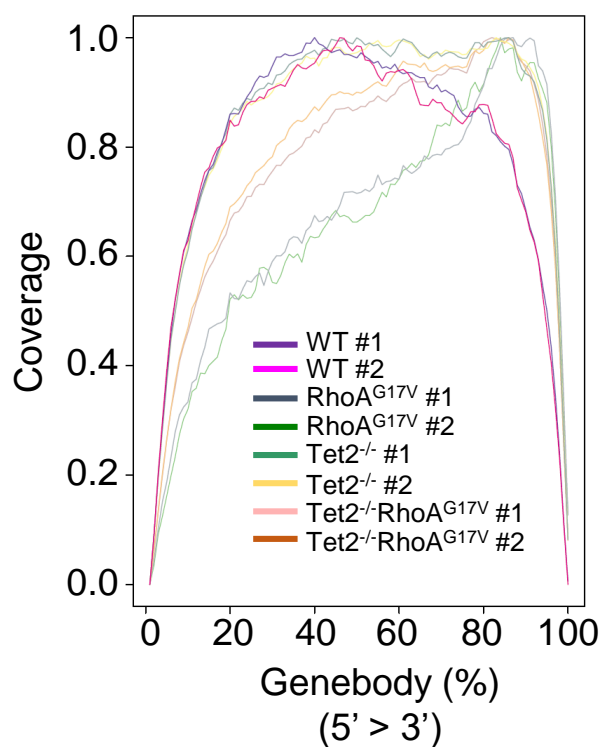
**A**

	Total	Mapped	Mapped Ratio	Unique Mapped	Unique Mapped Ratio
WT #1	125,446,268	66,240,938	52.80%	42,192,139	63.69%
WT #2	113,104,316	98,420,774	87.02%	58,686,837	59.63%
RhoA <sup>G17V</sup> #1	143,158,266	130,370,270	91.07%	57,856,978	44.38%
RhoA <sup>G17V</sup> #2	141,263,684	114,208,711	80.85%	48,877,769	42.80%
Tet2 <sup>-/-</sup> #1	156,874,372	128,908,844	82.17%	95,717,351	74.25%
Tet2 <sup>-/-</sup> #2	129,841,216	106,977,276	82.39%	79,760,491	74.56%
Tet2 <sup>-/-</sup> -RhoA <sup>G17V</sup> #1	154,789,692	131,583,982	85.01%	71,214,447	54.12%
Tet2 <sup>-/-</sup> -RhoA <sup>G17V</sup> #2	179,417,082	145,097,680	80.87%	80,074,784	55.19%

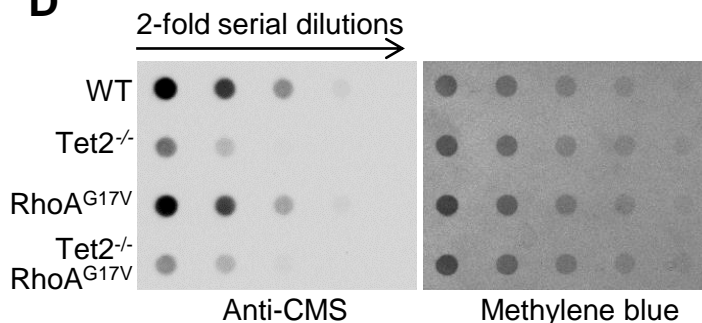
**B**



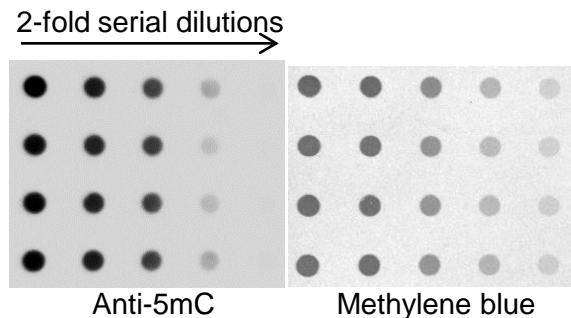
**C**



**D**



**E**



**Supplementary Figure 4, related to Figure 4. Changes in gene expression and DNA hydroxymethylation in WT and mutated CD4<sup>+</sup> T cells.**

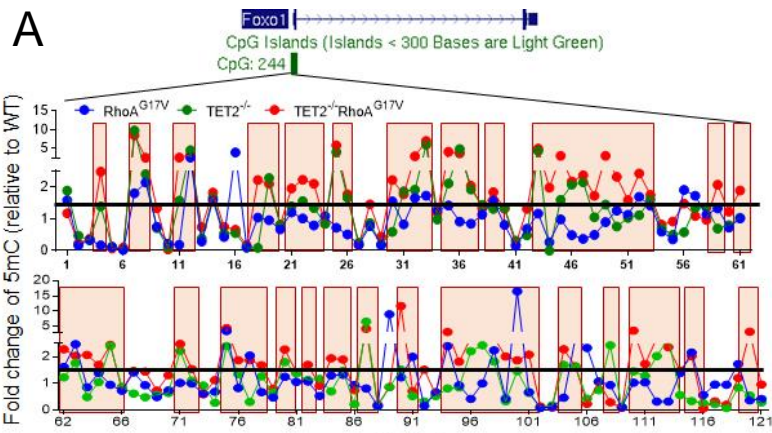
**(A)** Summary of RNA-Seq reads numbers and the mapping efficiency for each sample.

**(B)** Pearson's correlation between biological replicates of RNA-seq samples used to generate the gene expression datasets.

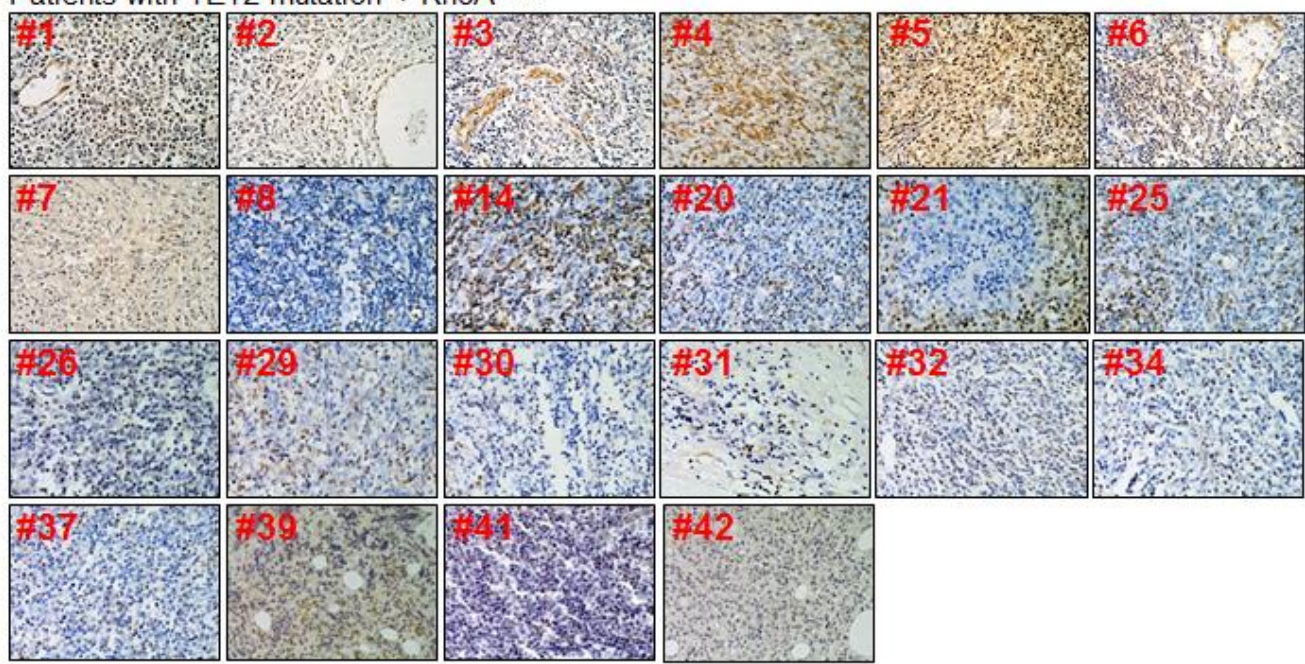
**(C)** The coverage of mapped RNA sequencing reads on all genes annotated in the UCSC genome browser.

**(D-E)** Dot-blot assay measuring the global 5hmC **(D)** and 5mC **(E)** levels in Thy1.2<sup>+</sup>GFP<sup>+</sup>CD4<sup>+</sup> T cells isolated from recipient mice transferred with WT, RhoA<sup>G17V</sup>, Tet2<sup>-/-</sup>, or Tet2<sup>-/-</sup>RhoA<sup>G17V</sup> T cells (20 weeks after adoptive transfer). Methylene blue staining was used to visualize the proper loading and dilutions of DNA amounts among the four groups.

Figure S5



**B** Patients with TET2 mutation + RhoA<sup>G17V</sup>



Patients with TET2 mutation

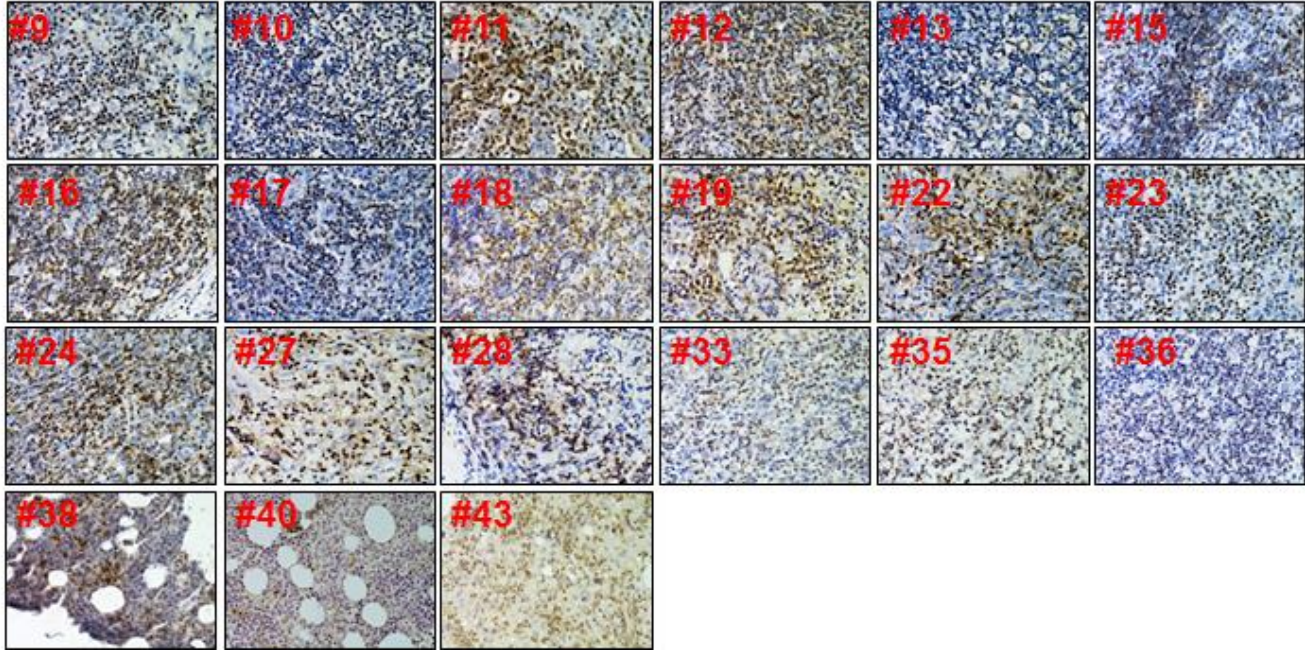
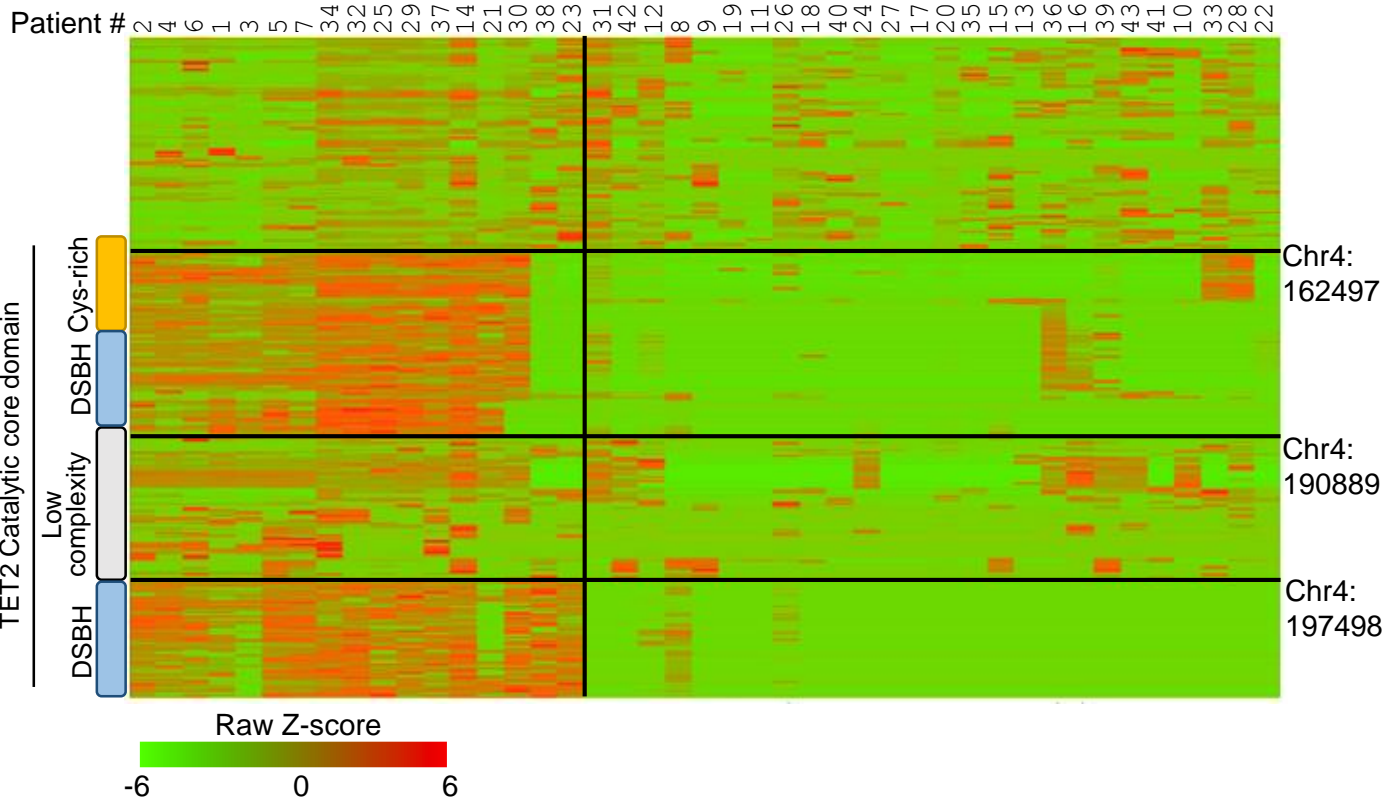
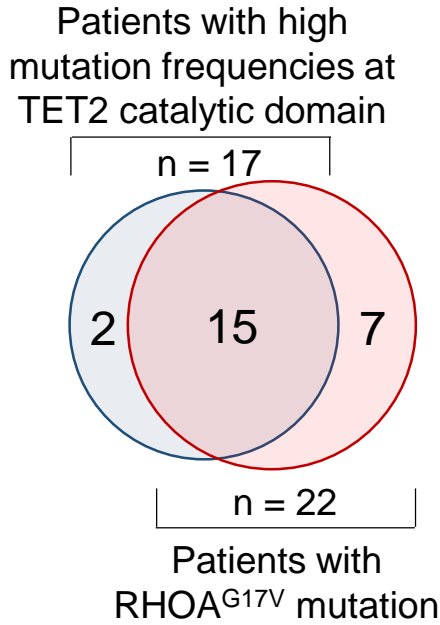


Figure S5 (continued)

C



D



**Supplementary Figure 5, related to Figure 6. DNA methylation status of one CpG island in the FoxO1 promoter region and FoxO1 staining results in AITL tumor samples.**

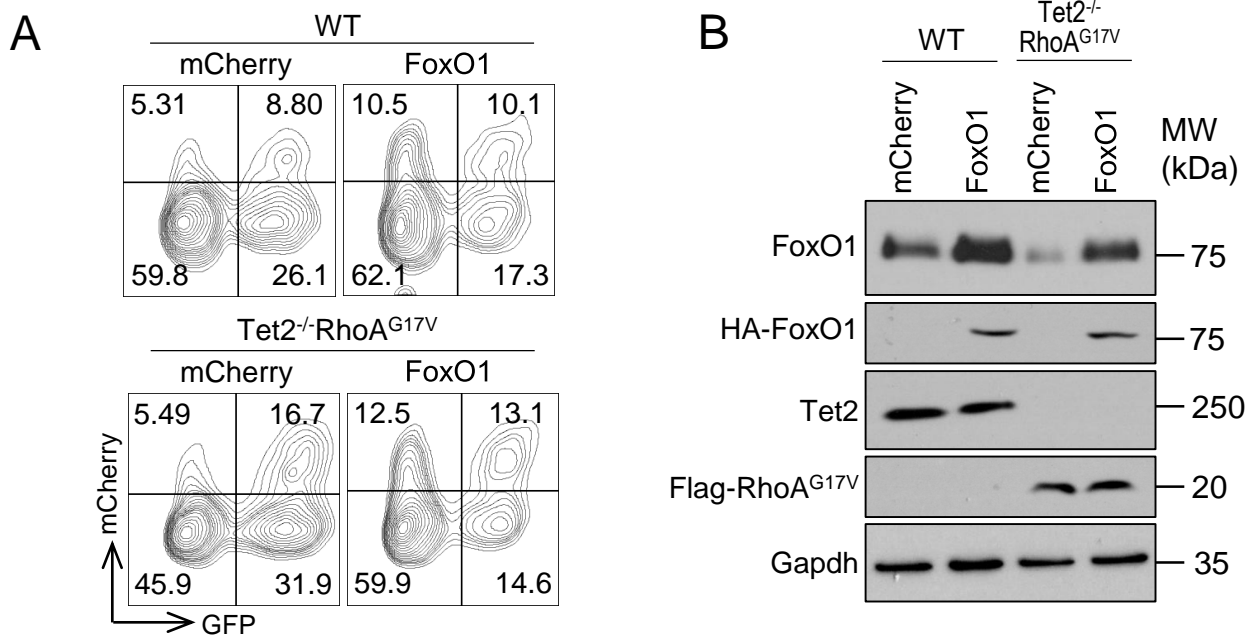
**(A)** Fold-changes of 5mC levels (relative to WT) in the indicated groups of CD4<sup>+</sup>GFP<sup>+</sup> cells following *in vitro* activation. CpG sites exhibited over 1.5-fold increase in DNA methylation in the Tet2<sup>-/-</sup> and / or Tet2<sup>-/-</sup>RhoA<sup>G17V</sup> groups were highlighted in red boxes.

**(B)** Representative images of FOXO1 IHC staining from 43 AITL patients. Top: Patients with both TET2 and RHOA mutations (Note: the seemingly strong IHC staining for samples 4/5/7 was due to increased staining of cytosolic FOXO1); Bottom: Patients with TET2 mutations alone. [Some of the same patient images were also presented in Figure 5F.](#)

**(C)** Heatmap showing mutation frequencies of TET2 in 43 AITL patients. Each column represents one AITL patient, each line represents a mutated genomic site. Patients were clustered based on TET2 mutation status. TET2 domain architecture was shown on the left. 17 AITL patients exhibited high mutation frequencies at the catalytic domain of TET2, while others had relatively low mutation frequencies at the same region of TET2.

**(D)** Venn diagram illustrating the overlap between patients with high mutation frequencies within the TET2 catalytic domain and patients with the RHOA<sup>G17V</sup> mutation.

# Figure S6



**Supplementary Figure 6, related to Figure 6. Re-expressing FoxO1 restored Tet2<sup>-/-</sup>RhoA<sup>G17V</sup>-induced disruption on CD4<sup>+</sup> T cell function.**

**(A)** Flow cytometry analysis of retroviral transduction efficiency in WT and Tet2<sup>-/-</sup> CD4<sup>+</sup> T cells transduced with GFP, mCherry, Flag-RhoA<sup>G17V</sup>-IRES-GFP, or HA-FoxO1-IRES-mCherry.

**(B)** Immunoblot analysis confirming the expression of FoxO1 and RhoA<sup>G17V</sup> in transduced WT and Tet2<sup>-/-</sup> CD4<sup>+</sup> T cells. Gapdh serves as loading control.